Bull. Mater. Sci. (2018) 41:68
https://doi.org/10.1007/s12034-018-1597-z

Microstructure and mechanical properties of carbon fibre-reinforced alumina composites fabricated from sol

CHAOYANG FAN, QINGSONG MA* and KUANHONG ZENG
Science and Technology on Advanced Ceramic Fibers and Composites Laboratory, National University of Defense Technology, Changsha 410073, People's Republic of China
*Author for correspondence (nudtmqs1975@163.com)

MS received 21 September 2017; accepted 17 October 2017; published online 17 May 2018

Abstract. Alumina matrix composites reinforced with the laminated and stitched carbon fibre cloth preform were fabricated through the infiltration–drying–heating route using the Al_2O_3 sol with a high solid content as raw materials. The investigation was focussed on the characteristics of sol and the mechanical properties and high-temperature resistance of C/Al_2O_3 composites. α-Al_2O_3 with favourable sintering activity can be obtained after heat treatment of sol at 1200°C. The as-received C/Al_2O_3 composites with a total porosity of 16.8% exhibit a flexural strength of 271.3 MPa and a notch toughness of 13.0 MPa $m^{1/2}$, respectively. As a result of the evolution of interface and matrix, the flexural strength of C/Al_2O_3 composites is decreased by 28.5% after heat treatment at 1600°C for 1 h under inert atmosphere. At the same time, fracture mode of composites is transformed from tough to brittle behaviour.

Keywords. Alumina; composites; carbon fibre reinforcement; sol; mechanical properties.

1. Introduction

Alumina (Al_2O_3) ceramics have attracted much interest for structural and functional applications owing to outstanding general properties [1–3]. However, brittle fracture problem should be resolved before its wide applications as structural materials. Continuous fibre with outstanding damage tolerance was considered to be the best reinforcement.

So far, oxide fibre was paid the most attention for reinforcing Al_2O_3 ceramics [4]. Oxide/Al_2O_3 composites can be used at 1100°C for a long time and at 1300°C for a short time, which is decided by high temperature resistance of oxide fibre [5]. Due to high price and large diameter of SiC fibre, SiC/Al_2O_3 composites are rarely reported [6,7]. There are not many studies on carbon fibre-reinforced Al_2O_3 composites [8–12], although carbon fibre was extensively employed to reinforce non-oxide ceramics. Apart from reaction-bonding aluminium oxide (RBAO) [6,7], sol–gel [8,11,12] and electrophoretic deposition (EPD) [13]; slurry impregnation and heat treatment (SIH) [4,9,10] are dominant routes to prepare fibre-reinforced Al_2O_3 composites.

Thanks to flexibility in structure design, desirable comprehensive performance and adaptability to complex shape, three-dimensional (3D) fibre preform was extensively adopted to fabricate composites for applications in astronautic and aeronautic equipments. To prepare 3D fibre-reinforced Al_2O_3 composites, especially large-size complex parts, gas infiltration and solution impregnation are preferred for the sake of homogeneous distribution of matrix and low fabrication temperature. At present, for the deposition of Al_2O_3, there is no proper gaseous raw material. As a result of large-size particles i.e., prone to sedimentation, 3D fibre-reinforced Al_2O_3 composites with heterogeneous distribution of matrix are fabricated through SIH route at high temperature [10]. When Al-containing solution was selected as a raw material, the transformation efficiency from solution via gel to Al_2O_3 is very low, creating 3D fibre-reinforced Al_2O_3 composites with high porosity and low strength [8,11,12,14].

Recently, 3D fibre-reinforced mullite, ZrO_2–SiO_2 and SiO_2 composites were fabricated through the route of sol impregnation–drying–heat treatment (SIDH) using sols with high solid content (20∼25 wt%) as raw materials [15–20]. These studies indicate that SIDH route improves fabrication efficiency of solution impregnation route and reserves its advantages of homogeneous distribution of matrix and low fabrication temperature. In this study, processing, microstructures and mechanical properties of 3D carbon fibre-reinforced Al_2O_3 (C/Al_2O_3) composites prepared via SIDH route were reported.

2. Experimental

2.1 *Raw materials and processing*

The reinforcement was 3D carbon fibre (T300 3k, ex-PAN carbon fibre, Toray) preform with a fibre volume fraction of 35% and a fibre density of 1.76 g cm^{-3}. The structure of preform was laminated and stitched carbon fibre cloth. The raw material for matrix was an alumina sol with a

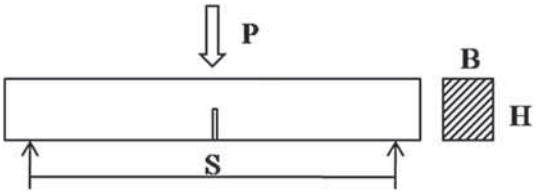

Figure 1. Sketch map of fracture toughness testing method.

solid content of 30 wt% and a colloid particle diameter of 20∼30 nm.

Carbon fibre preform was heated at 1400°C for 1 h to remove surface size, followed by vacuum impregnation of sol. After soaked in sol for 6 h, preform was dried at 200°C for 4 h and then, heated at preset temperature for 1 h in inert atmosphere with a heating rate of 10°C min^{-1}. The cycle of vacuum impregnation–drying–heat treatment was repeated to densify composites. When the weight gain of composites was <1%, the fabrication of C/Al_2O_3 composites was accomplished. During densification, heat treatment was carried out at 1100°C, if the weight gain of composites was >3% and at 1400°C, if the weight gain of composites was <3%.

2.2 *Characterization methods*

The gel powders that were obtained by drying sol at 200°C were heated at different temperatures. Then, phase composition of powders was determined by X-ray diffraction, which was carried out on a diffractometer (Bruker D8 advance) with CuKα radiation. Data were digitally recorded during a continuous scan in the range of angle (2θ) from 10 to 80° with a scanning rate of 4° min^{-1}. At the same time, the gel powders were cold-pressed at 120 MPa to form wafer. After heat treatment at different temperatures, linear shrinkage and microstructure of the wafer were measured and observed.

Apparent density (ρ_a) of as-received C/Al_2O_3 composites was computed from the weight-to-volume ratio. The bulk density and open porosity were measured according to Archimedes' principle with deionized water as immersion medium. The true density (ρ_m) of matrix was measured on powdered sample using a pycnometer. Then, the theoretic density (ρ_T) of C/Al_2O_3 composites was calculated from the equation:

$$\rho_T = V_f \times \rho_f + V_m \times \rho_m, \quad (1)$$

where V_f and V_m are volume fractions of fibre and matrix, ρ_f and ρ_m are densities of fibre and matrix, respectively. Thus, total porosity was equal to $1 - (\rho_a/\rho_T)$ and open porosity subtracted from total porosity gives close porosity.

The as-received C/Al_2O_3 composites were annealed in high purity Ar atmosphere at 1600°C for 1 h to characterize its thermal stability. Three-point bending test was employed to evaluate flexural strength of composites with a span/height ratio of 15 and a cross-head speed of 0.5 mm min^{-1}. As shown in figure 1, the notch toughness was determined by the single edge notched beam (SENB) method with a sample size of 40 mm × 8 mm (H) × 4 mm (B) and a cross-head speed of 0.05 mm min^{-1}. The span (S) was 32 mm. The notch was cut by programme-controlled diamond blade, followed by size measurement under microscope. The notch width was 0.28 mm and the ratio of notch depth (a) to specimen height (H) was 0.496. The notch toughness (K_{nt}) was calculated according to the equation [21]:

$$K_{nt} = \left[(PS)/BH^{3/2}\right] \times f(a/H), \quad (2)$$

where $f(a/H) = 2.9(a/H)^{1/2} - 4.6(a/H)^{3/2} + 21.8(a/H)^{5/2} - 37.6(a/H)^{7/2} + 38.7(a/H)^{9/2}$ and P was the maximum load. Five specimens were tested to obtain the average flexural strength and notch toughness. Scanning electron microscopy (SEM, Quanta-200 EDAX) was employed to observe microstructures of wafers and composites.

3. Results and discussion

3.1 *Characteristics of sol*

Phase compositions of gel powders at various temperatures after heat treatment are presented in figure 2. Only faint diffraction peaks of γ-Al_2O_3 are found before 1100°C. At 1100°C, α-Al_2O_3 phase which is transformed from γ-Al_2O_3 is detected, although its diffraction peaks are not obvious. All sharp-pointed diffraction peaks can be assigned to α-Al_2O_3 phase at 1200°C, indicating complete transformation of γ-Al_2O_3. Crystallization of α-Al_2O_3 is enhanced with increasing the temperature to 1400°C, as reflected by the elevated intensity and sharpness of diffraction peaks.

Linear shrinkage of gel powder wafers at various temperatures after heat treatment is shown in figure 3. A linear shrinkage of 16.8% is observed at 800°C. This value is enlarged with increasing the temperature, displaying 18.2% at 1000°C and 24.3% at 1200°C, respectively. Low crystallinity of gel powder before 1200°C is responsible for the high sintering activity. The obvious crystallization of α-Al_2O_3 at 1200°C reduces sintering activity of gel powder, leading to minute increase in linear shrinkage at 1400°C (24.5%). However, the driving force for solid state sintering of α-Al_2O_3 is high enough at 1600°C. Thus, linear shrinkage is further increased to 29.2%. Due to the notable sintering shrinkage, a compact fracture surface of gel powder wafer after heat treatment at 1400°C is observed in figure 4. It is noted that micrometre grains bond tightly with each other, which is beneficial to mechanical properties.

3.2 *Microstructure and mechanical properties of 3D C/Al_2O_3 composites*

The true density (ρ_m) of the matrix was measured as 3.80 g cm^{-3} and the theoretic density (ρ_T) of composites was

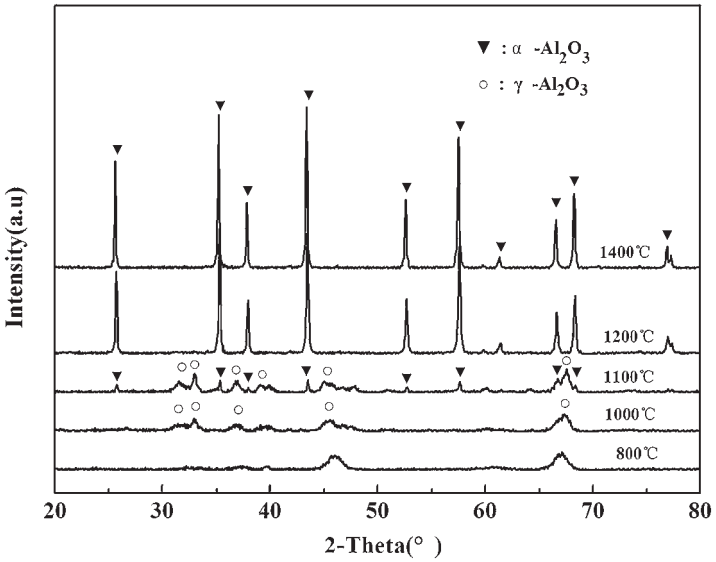

Figure 2. XRD patterns of gel powders after heat treatment at different temperatures.

calculated as 3.09 g cm^{-3}. Thus, C/Al_2O_3 composites with a total porosity of 16.8% were obtained since the apparent density of composites was measured as 2.57 g cm^{-3}. An open porosity of 13.3% was verified by Archimedes' principle. Hence, the close porosity of composites was 3.5%.

SEM appearances of as-received C/Al_2O_3 composites are presented in figure 5. As shown, a comparatively uniform distribution of matrix is realized without large pores and cracks. The inter- and intra-bundle spaces in preform are effectively filled and the mono-fibres are well surrounded by matrix. The microstructure is formed due to low viscosity and nanometre size of sol. In early stages, it is easy for sol to impregnate into spaces in preform. Space size is reduced with increasing the density of composites. Simultaneously, the diffusion channels to space become narrow and wandering. Thus, it is more and more difficult for sol to diffuse into composites during late stages, resulting in some micropores. At the same time, microcracks are observed as a result of thermal expansion mismatch between fibre and matrix.

The flexural strength and notch toughness of as-received composites are 271.3 ± 46.1 MPa and 13.0 ± 2.8 MPa $m^{1/2}$, respectively. The mechanical properties are satisfying with regard to absence of interfacial coating and a total porosity of 16.8%. In figure 6a, a maximum displacement of ∼1.1 mm at invalidation point and circuitous decline of load after this point are observed. Figure 7 shows extensive fibre pull-out and long pull-out length. The non-catastrophic fracture behaviour demonstrates the prominent toughening effect of continuous fibre reinforcement.

After annealed at 1600°C for 1 h under inert atmosphere, C/Al_2O_3 composites show a flexural strength of 194.1 MPa, which is 71.5% that of as-received composites. It is clear from figure 6b that the annealed composites show a maximum

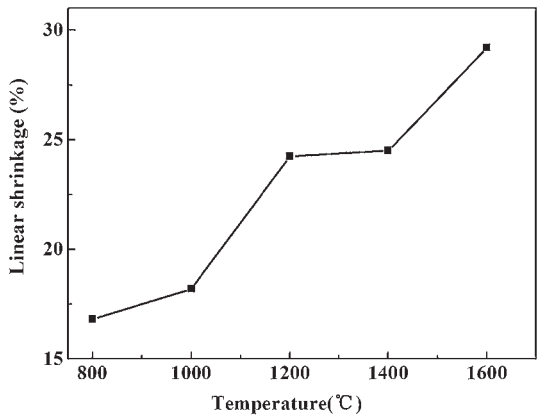

Figure 3. Linear shrinkage of gel powder wafers after heat treatment at various temperatures.

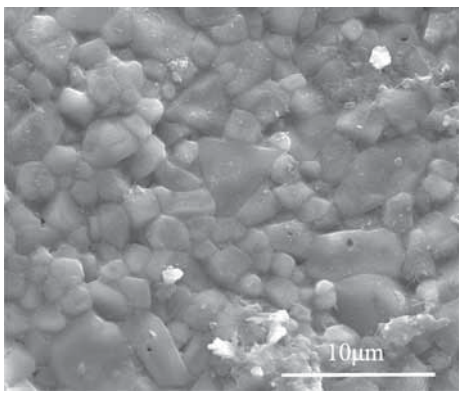

Figure 4. Fracture surface of gel powder wafer after heat treatment at 1400°C.

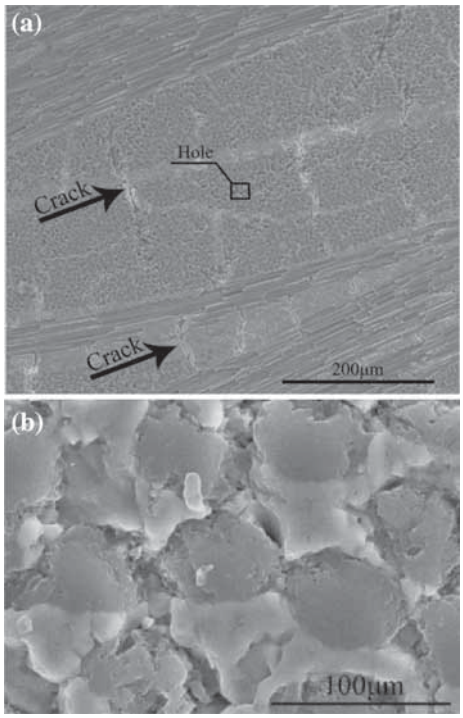

Figure 5. Cross-section morphology of as-received C/Al_2O_3 composites.

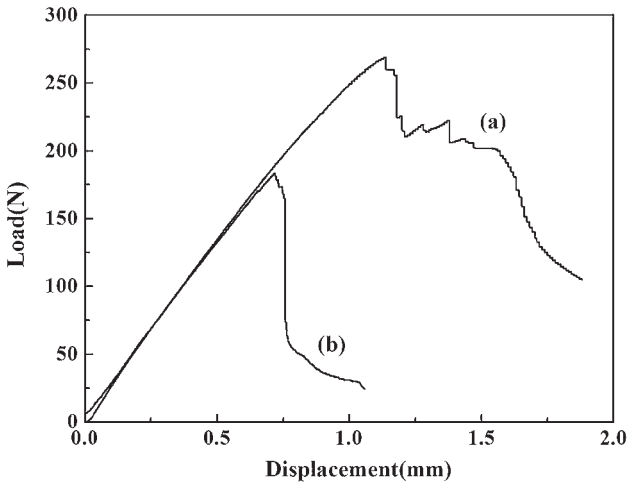

Figure 6. The representative load–displacement curves of C/Al_2O_3 composites: (**a**) as-received and (**b**) after annealing.

displacement of ∼0.7 mm at invalidation point and vertical decline of load after this point. The conversion from tough to brittle fracture behaviour indicates that interfacial bonding is enhanced after heat treatment at 1600°C.

The heat treatment at 1600°C promotes further sintering densification of matrix since an obvious increase of linear shrinkage from 24.5% at 1400°C to 29.2% at 1600°C is observed in figure 3. This sintering shrinkage strengthens the physical bonding between fibre and matrix.

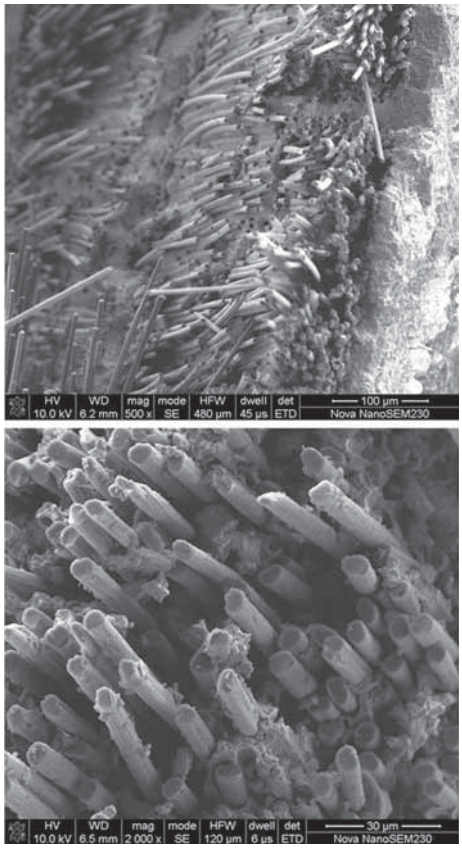

Figure 7. Fracture surface of C/Al_2O_3 composites.

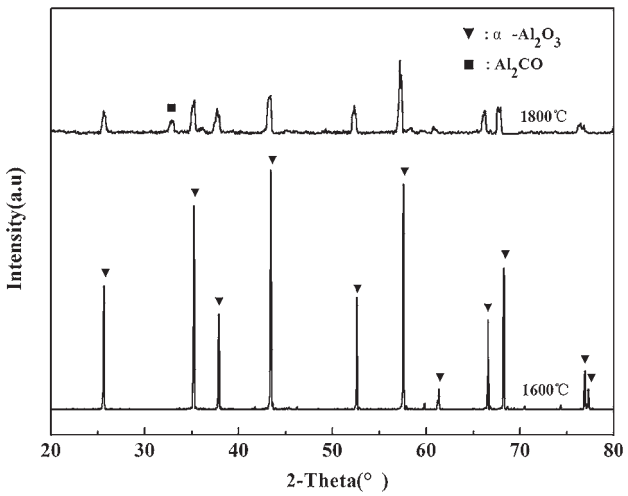

Figure 8. XRD patterns of Al_2O_3 powders after heat treatment at 1600 and 1800°C.

When gel powder wafers were heated at 1800°C for 1 h in high purity Ar, a new Al_2CO phase is detected in figure 8 and deep dark appearance is observed in figure 9. The reaction between active carbon atmosphere in graphite furnace and α-Al_2O_3, is supposed to explain this phenomenon. For C/Al_2O_3 composites, it is very likely that the amorphous active carbon on fibre surface derived from decomposition

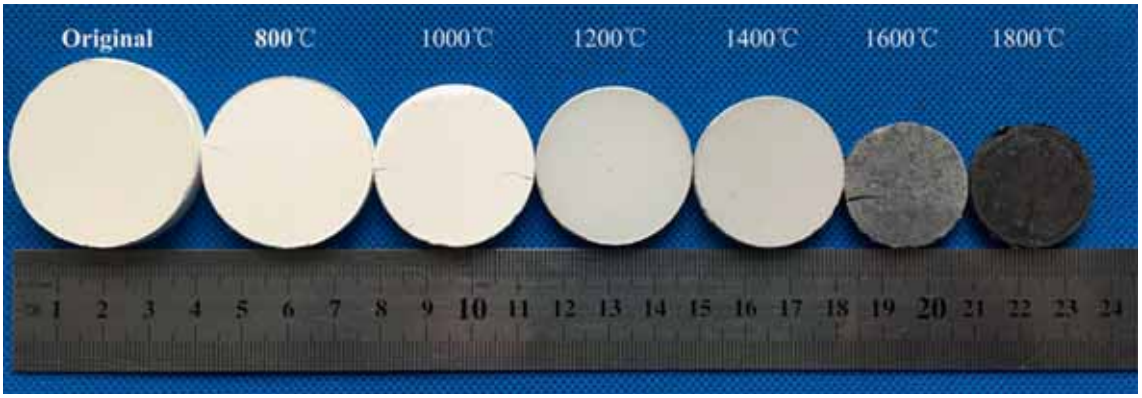

Figure 9. Optical photos of gel powder wafers after heat treatment at various temperatures.

of surface size would react with matrix at this temperature. After heat treatment at 1800°C for 1 h, C/Al_2O_3 composites showed a weight loss of only 0.77%, implying a slight reaction between carbon and Al_2O_3.

At 1600°C, a darkish wafer was obtained (figure 9) and a weight loss of 0.34% of C/Al_2O_3 composites was found, suggesting occurrence of the reaction between carbon and Al_2O_3. The reaction is considered to be slighter because of the absence of Al_2CO phase in figure 8 and much less weight loss. However, tensile strength loss of carbon fibre and strong interfacial bonding are created due to the slight reaction, leading to degradation in flexural strength and fracture toughness of composites. So, interfacial coating is necessary to improve mechanical properties and thermal stability of C/Al_2O_3 composites. This will be focussed in subsequent studies.

4. Conclusion

An Al_2O_3 sol with high solid content was used to fabricate C/Al_2O_3 composites. After heat treatment at 1200°C, α-Al_2O_3 with favourable sintering activity was obtained. 3D carbon fibre-reinforced Al_2O_3 composites with a total porosity of 16.8% were fabricated via vacuum impregnation–drying–heat treatment route, exhibiting 271.3 MPa in flexural strength and 13.0 MPa $m^{1/2}$ in notch toughness. After annealing at 1600°C for 1 h under inert atmosphere, C/Al_2O_3 composites display degradation in flexural strength and transformation of fracture behaviour from tough to brittle mode.

Acknowledgements

This work was financially supported by the Science Innovation Foundation of Shanghai Academy of Spaceflight Technology (Grant No. SAST2015043).

References

[1] Satapathy L N and Swaroop S 2005 *Bull. Mater. Sci*. **28** 281
[2] Mallik A K, Gangadharan S, Dutta S and Basu D 2010 *Bull. Mater. Sci*. **33** 445
[3] Tan H B, Ma X L and Fu M X 2013 *Bull. Mater. Sci*. **36** 153
[4] Zok F W 2006 *J. Am. Ceram. Soc*. **89** 3309
[5] Volkmann E, Tushtev K, Koch D, Wilhelmi C, Göring J and Rezwan K 2015 *Compos. Part A* **68** 19
[6] Wilshire B and Carreño F 2000 *J. Eur. Ceram. Soc*. **20** 463
[7] Llorca J, Elices M and Celemin J A 1998 *Acta Mater.* **46** 2441
[8] Chen Z F, Zhang L T, Cheng L F, Xu Y D and Han G F 2003 *J. Inorg. Mater*. **18** 638 (in Chinese)
[9] Colomban Ph and Wey M 1997 *J. Eur. Ceram. Soc*. **17** 1475
[10] Liu H K and Lin B H 2001 *Mater. Lett*. **48** 230
[11] Chen Z F, Zhang L T, Cheng L F, Xu Y D and Xiao P 2001 *J. Aeronaut. Mater*. **21** 28 (in Chinese)
[12] Xie Z F, Xiao J Y, Chen Z H, Wang X Y, Zheng W W and Jiang D Z 1998 *J. Nat. Univ. Defense Technol.* **20** 14 (in Chinese)
[13] Stoll E, Mahr P, Krüger H G, Kern H, Thomas B J C and Boccaccini A R 2006 *J. Eur. Ceram. Soc*. **26** 1567
[14] Naskar M K, Chatterjee M, Dey A and Basu K 2004 *Ceram. Int*. **30** 257
[15] Wang Y, Liu H T, Cheng H F and Wang J 2014 *Mater. Lett*. **126** 236
[16] Wang Y, Cheng H F and Wang J 2014 *Ceram. Int*. **40** 4707
[17] Wang Y, Liu H T, Cheng H F and Wang J 2013 *Ceram. Int*. **39** 9229
[18] Xiang Y, Wang Q, Cao F, Ma Y W and Quan D L 2017 *Ceram. Int*. **43** 854
[19] Wang Q, Cao F, Xiang Y and Peng Z H 2017 *Ceram. Int*. **43** 884
[20] Liu H T, Ma Q S and Liu W D 2014 *Ceram. Int*. **40** 7203
[21] Guan Z D, Zhang Z T and Jiao J S 1992 (eds) *Physical properties of inorganic materials* (Beijing: Tsinghua University Press) (in Chinese)